Geometrical Synthesis of Offset Reflector Antennas Using Local Axis-Displaced Quadric Surfaces

R. A. Penchel[1], J. R. Bergmann[1] and F. J. S. Moreira[2]
[1] Center for Telecommunications Studies, PUC-Rio, Rio de Janeiro, RJ, Brazil, {rapenchel, bergmann}@cetuc.puc-rio.br
[2] Dept. Electronics Engeneering, UFMG, Belo Horizonte, MG, Brazil, fernandomoreira@ufmg.br

Abstract — **This work investigates an alternative numerical procedure for the geometrical synthesis of offset reflector antennas with an arbitrary radiation pattern in the far-field region according to geometrical optics. The method uses local axis-displaced confocal quadric surfaces to describe the shaped reflector. In this approach, a nonlinear operator must be solved as a boundary value problem. To illustrate the method, we have chosen an offset configuration with a circular contour coverage and Gaussian power density. The results were validated by the physical optics approximation.**

Index Terms **— offset antenna, Monge-Ampère, confocal quadric surface.**

I. INTRODUCTION

The synthesis of circularly symmetric dual-reflector antennas based on the combination of local conic sections has been investigated [1]–[3]. It was shown that few conic sections are needed to accurately represent the shaped reflector generatrix. In [2] the technique presented in [1] was generalized to various axially symmetric configurations, and recently extended to dual-reflector antennas with omnidirectional coverage and arbitrary radiation pattern in the elevation plane [3]. In [2] and [3] it was shown that the synthesis technique based on local conic sections is numerically efficient and has better convergence rates than those techniques based on the solution of ordinary differential equations.

The present problem is to determine, under Geometrical Optics (GO) principles, a shaped offset reflector which scatters an arbitrary radiation pattern when illuminated by a point source, as illustrated in Fig. 1. The exact theoretical formulation for this problem was studied by Westcott in [4] and [5], and involves the numerical evaluation of a second order nonlinear partial differential equation of Monge-Ampère type, subject to a nonlinear boundary condition. Problems involving offset dual-reflector antennas [6], [7] and, more recently, the synthesis of three-dimensional dielectric lenses [8] lead to similar Monge-Ampère equations.

The numerical schemes used in [4]–[8] adopt finite differences to approximate derivatives and linearization of a set of nonlinear equations, iteratively solved by Newton's or similar methods. If convergence is achieved, the solution is given as a finite number of points defining the reflecting (or refracting) surface. The problem which remains is the exponential growth of discretization error in the central portion of polar grids where a singularity is present. In [7], an alternative method that solves the problem with a complex rectangular grid is investigated, but it generates another problem at the edges, where the difficulty in describing the contour is greater.

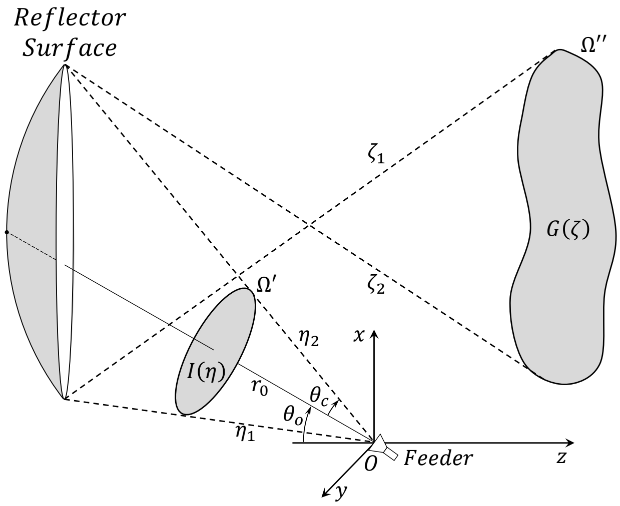

Fig. 1. Geometry of the offset reflector antenna

In this work, the idea exploited in [1]–[3] is extended to the GO synthesis of offset reflector antennas. Unlike in axially symmetric configurations, where conic sections were used to represent the surface generatrix, here axis-displaced confocal quadrics are used to describe the shaped offset reflector.

II. GEOMETRICAL SYNTHESIS PROBLEM

As illustrated in Fig. 1, the synthesis problem considers a reflector illuminated by a point source with phase center at the origin and radiation pattern $I(\eta)$. From GO principles, all incident energy is reflected within a far-field region Ω'' where power density is described by the function $G(\zeta)$. To present the formulation, it is convenient to adopt a complex notation widely used in [5]–[7], where, by stereographic projection, the incident rays directions are defined, as functions of the spherical coordinates θ and ϕ, by

$$\eta = \cot(\theta/2)\, e^{i\phi} \tag{1}$$

and reflected rays directions, as functions of the spherical coordinates α and β, by

$$\zeta = \cot(\alpha/2)\, e^{i\beta} \tag{2}$$

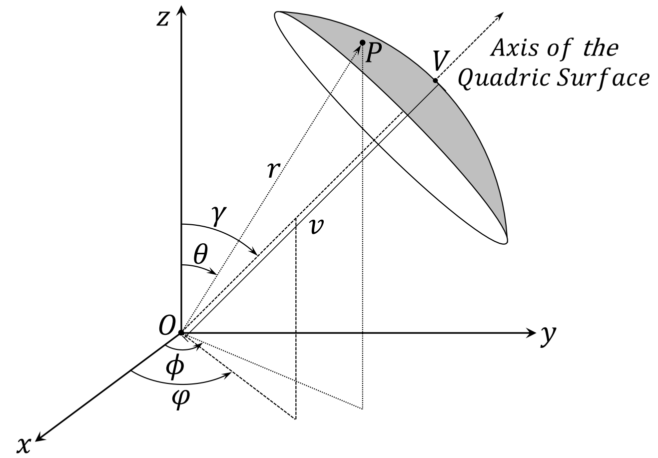

Fig. 2. Local axis-displaced confocal quadric surface

From a GO perspective, a set of rays departing from the feeder (with radiation pattern $I(\eta)$ and limited by the contour Ω', is mapped at the region limited by contour Ω'', where the radiation pattern is described by $G(\zeta)$. The mapping transformation $\tau{:}\,\eta \rightarrow \zeta$ is obtained by imposing Snell's law and conservation of energy. The first relates incident (η) and reflected (ζ) directions through the following partial differential equation [5]:

$$L_\eta = \frac{1}{\zeta - \eta} \tag{3}$$

where L is the real mapping function given by

$$r = e^{L(\eta)}(|\eta|^2 + 1) \tag{4}$$

and r is the distance from the feeder to the reflector along the optical path.

The conservation of energy imposes that the mapping τ has to alter the solid angle of the reflected beam by the ratio I/G. In the main coordinate system in complex notation [5]:

$$\left|\zeta_\eta\right|^2 - \left|\zeta_{\bar{\eta}}\right|^2 = \pm \frac{I(\eta)}{G(\zeta)} \left(\frac{1 + |\zeta|^2}{1 + |\eta|^2}\right)^2 \tag{5}$$

where $\bar{\eta}$ is complex conjugate of η. From (3) and (5) one obtains the mapping τ as a Monge-Ampère differential equation [5]:

$$\left|L_{\eta\eta} - L_\eta^2\right|^2 - \left|L_{\eta\bar{\eta}}\right|^2 = \pm \frac{I(\eta)}{G(\zeta)} \left(\frac{1 + |\zeta|^2}{1 + |\eta|^2}\right)^2 \left|L_\eta\right|^4 \tag{6}$$

III. Numerical Method

Several works in the literature use a generalization of Newton's method with an approximate Finite Difference (FD) scheme to solve the Monge-Ampère equation under a given boundary condition [4]–[8]. For a polar grid, the FD approximations for first and second order derivatives lead to a discretization error that grows exponentially toward the center of the grid. To reduce such errors, it is assumed that the reflector surface can be locally represented by axis-displaced confocal quadric surfaces. The advantage of this treatment is that it uses the exact analytical forms of the derivatives in the Monge-Ampère equation, reducing discretization errors. It was considered elliptic form of (6), where signal is negative [5].

A. Axis-Displaced Confocal Quadric Surface

The axis-displaced confocal quadric surface is obtained by the rotation of a conic section around its axis. It is described in spherical coordinates by

$$r = \frac{a}{b \sin\theta \cos\phi + c \sin\theta \,\mathrm{sen}\, \phi + d \cos\theta - 1} \tag{7}$$

or, in complex notation [6],

$$a e^{-L(\eta)} = (d-1)\eta\bar{\eta} + (b - ic)\eta + (b + ic)\bar{\eta} - d - 1 \tag{8}$$

where

$$a = -ev \tag{9–a}$$

$$b = e \sin\gamma \cos\varphi \tag{9–b}$$

$$c = e \sin\gamma \sin\varphi \tag{9–c}$$

$$d = e \cos\gamma \tag{9–d}$$

a is the semilatus rectum, e is the eccentricity, v is the distance between origin O and vertex V, φ is the azimuth angle, and γ is the elevation angle (see Fig. 2). By substituting (8) in (3), Snell's law for a confocal quadric surface is represented as:

$$\zeta = \frac{(d+1) - (b + ic)\bar{\eta}}{(b - ic) + (d-1)\bar{\eta}} \tag{10}$$

It can be noted in (10) that the relation between η and ζ is valid for any confocal quadric with the same parameters b, c, and d. For a confocal quadric to be uniquely specified, a (directly associated with v) must be defined.

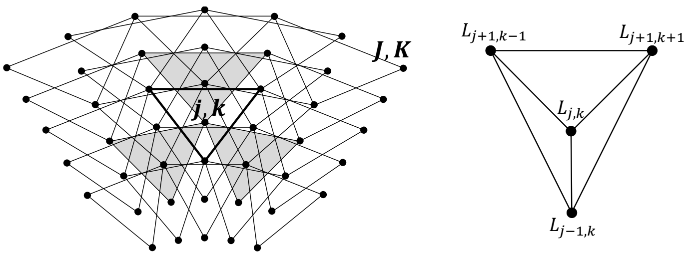

Fig. 3. (a) Triangular scheme (b) Local triangular cell

B. Nonlinear Operator

The real continuous function $L(\eta)$, solution of (6), describes the shaped reflector surface. From a numerical perspective, the solution of (6) is a finite set of values $L\left[L_{1,1}, \ldots L_{j,k}, \ldots, L_{J,K}\right]$ which are interpolated to mold a surface that approximates the original solution $L(\eta)$. As illustrated in Fig. 3, J and K are the number of rings and radials of the polar grid, respectively. Each value $L_{j,k}$ must be a local solution of the Monge-Ampère equation. Assuming that $L_{j,k}$ can be locally defined by a quadric described by (8), the Monge-Ampère equation (6) can be obtained by deriving (10) with respect to η and $\bar{\eta}$ and applying the results in (5). In an operator form:

$$\Gamma_{j,k}\left[b_{j,k},c_{j,k},d_{j,k}\right] = -\frac{I(\eta)}{G(\zeta)}\left(\frac{|\zeta|^2+1}{|\eta|^2+1}\right)^2 + \left|\frac{b_{j,k}^2+c_{j,k}^2+d_{j,k}^2-1}{\left[(d_{j,k}-1)\bar{\eta}+\left(b_{j,k}-ic_{j,k}\right)\right]^2}\right|^2 \quad (11)$$

Note that $\zeta_\eta = 0$ and, consequently, $\left|L_{\eta\eta} - L_\eta^2\right| = 0$, simplifying the mapping τ for a quadric surface.

As observed for (10), the solution of (11) is a family of quadric surfaces with the same parameters $b_{j,k}$, $c_{j,k}$, $d_{j,k}$. The choice of $a_{j,k}$ must be taken such that the neighbor quadric surfaces are continuous and the set of all quadrics form a continuous shaped reflector. To achieve that, we have adopted a triangular scheme associated with the regular polar grid where surface continuity is imposed over three adjacent quadric surfaces (see Fig. 3 (a)). To find $a_{j,k}$, $b_{j,k}$, $c_{j,k}$, and $d_{j,k}$, (8) is evaluated at four points of a local triangular cell (see Fig. 3(b)), leading to a 4x4 system of linear equations. So, the local confocal quadric parameters are functions of $L_{j-1,k}$, $L_{j,k}$, $L_{j+1,k-1}$ and $L_{j+1,k+1}$.

To start the iterative process, an initial solution ($L^{(0)}$) is required, which should be as close as possible of the desired solution to provide the convergence of the design technique. A good choice for $L^{(0)}$ is a confocal quadric obtained by imposing Snell's law for the two reflector-edge rays in the symmetry plane $\phi = 0$ (the rays illustrated in Fig. 1). For these two rays, (10) is rewritten as:

$$\begin{cases}(\zeta_1+\eta_1)b_{j,k}^{(0)} + (\eta_1\zeta_1 - 1)d_{j,k}^{(0)} = \eta_1\zeta_1 + 1\\(\zeta_2+\eta_2)b_{j,k}^{(0)} + (\eta_2\zeta_2 - 1)d_{j,k}^{(0)} = \eta_2\zeta_2 + 1\end{cases} \quad (12)$$

as $c_{j,k}^{(0)} = 0$ at the symmetry plane, $b_{j,k}^{(0)}$ and $d_{j,k}^{(0)}$ are directly calculated from (12) and $a_{j,k}^{(0)}$ is given by:

$$a_{j,k}^{(0)} = r_0\left(b_{j,k}\sin\theta_0 + d_{j,k}\cos\theta_0 - 1\right) \quad (13)$$

where r_0 is the distance between origin and reflector surface, θ_c and θ_0 are the feeder half-angle and offset angle, respectively, as illustrated in Fig. 1.

The iterative process starts by applying the quadric initial parameters $a_{j,k}^{(0)}$, $b_{j,k}^{(0)}$, $c_{j,k}^{(0)}$, $d_{j,k}^{(0)}$ into (11) for all values of η in the grid. If the operator value $\Gamma^{(0)}$ is greater than the convergence criterion, a new iteration must be done and the new solution ($L^{(1)}$) is obtained by:

$$\left[L^{(n+1)}\right] = \left[L^{(n)}\right] - \left[J^{(n)}\right]^{-1}\left[\Gamma^{(n)}\right] \quad (14)$$

where $J^{(n)}$ is the Frechet Derivative of operator $\Gamma^{(n)}$ of the n-th iteration. Note that $L^{(0)}$ and $\Gamma^{(0)}$ are already known and $J^{(0)}$ are obtain analytically deriving (11) with respect $L_{j-1,k}^{(0)}$, $L_{j,k}^{(0)}$, $L_{j+1,k-1}^{(0)}$and $L_{j+1,k+1}^{(0)}$. So, the linear system (14) is solved and a new solution ($L^{(1)}$) is obtained. From $L^{(1)}$, the local quadrics parameters $a_{j,k}^{(1)}$ $b_{j,k}^{(1)}$, $c_{j,k}^{(1)}$, $d_{j,k}^{(1)}$ are calculated solving a 4x4 linear system obtained by applying local triangular cell in (8).

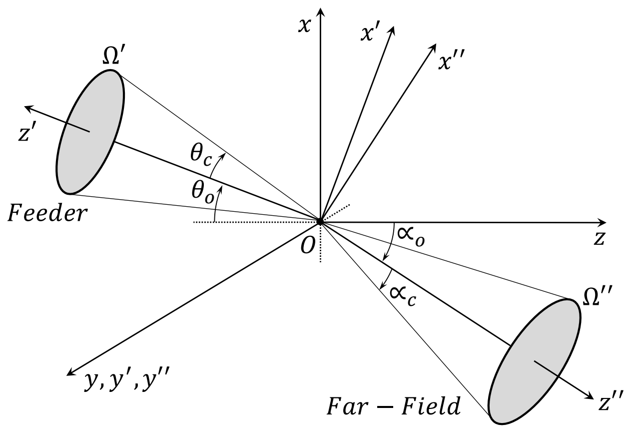

Fig. 4. Auxiliay coordinate systems

Again, the operator $\Gamma^{(1)}$ is evaluated and if greater than the convergence criterion this iterative process is repeated until the criterion is reached.

C. Boundary Conditions

Figure 4 shows the feeder and far-field radiation cones, where the primed ($'$) and double-primed ($''$) variables refer to the feeder and far-field coordinates, respectively. The relations between main (unprimed) and auxiliary systems are [6]:

$$\eta' = \frac{\eta_0\eta - 1}{\eta_0 - \eta} \quad ; \quad \zeta'' = \frac{\zeta_0\zeta - 1}{\zeta_0 - \zeta} \quad (15)$$

where

$$\eta_0 = \cot\left(\frac{\pi - \theta_0}{2}\right) \quad ; \quad \zeta_0 = \cot\left(\frac{\alpha_0}{2}\right) \quad (16)$$

and θ_0 and α_0 are the feeder and far-field offset angles, respectively, as illustrated in Fig. 4.

In this work we have adopted a circular boundary condition, represented by:

$$\left(\frac{\mathrm{Re}[\zeta'']}{\zeta_c}\right)^2 + \left(\frac{\mathrm{Im}[\zeta'']}{\zeta_c}\right)^2 = 1 \quad (17)$$

where

$$\zeta_c = \cot\left(\frac{\alpha_c}{2}\right) \quad (18)$$

α_c is the angular aperture of the reflected beam, as illustrated in Fig. 4. Rewriting (17) as an operator in the main coordinate system:

$$\Gamma_c\left[b_{j,k},c_{j,k},d_{j,k}\right] = \left|\frac{1}{\zeta_c}\left(\frac{\zeta_0\zeta - 1}{\zeta_0 - \zeta}\right)\right|^2 - 1 \quad (19)$$

IV. Design Analysis

To evaluate synthesis procedure described in Sects. II and III, we explore a case study where an offset reflector antenna was shaped to provide, according to GO principles, a Gaussian radiation pattern in a circular cone described by:

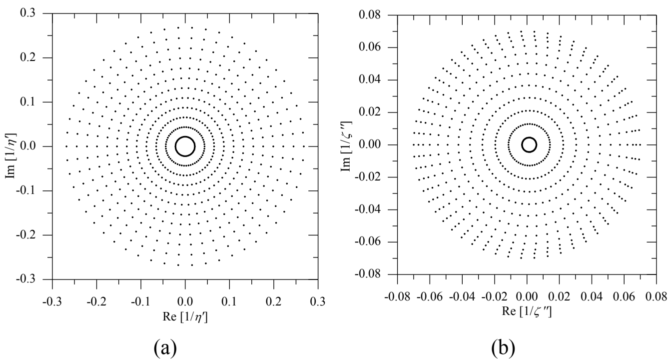

Fig. 5. Representation of ray directions of the (a) feeder (complex plane η') and (b) far-field (complex plane ζ'')

$$G(\alpha'') = G_0 e^{-\psi|\cot(\alpha''/2)|} \tag{20}$$

where G_0 is a normalization constant. The feeder radiation pattern was modeled by $\cos^{2n}\theta'$, where $n = 9.6$, half-angle $\theta_c = 30°$, and offset angle $\theta_0 = 50°$, providing a 12 dB attenuation at the reflector edge. The offset reflector antenna was synthesized to radiate a circular cone with $\alpha_0 = -18°$, half-angle $\alpha_c = 8°$, and Gaussian far-field pattern with $\psi = 0.69$, corresponding to a 3 dB attenuation at the contour. The distance v was adjusted to provide a reflector with a diameter of 4 meters. Figure 5 (a) shows the feeder polar grid in the complex plane η', defined with $J = 12$ rings and $K = 54$ radials. Figure 5 (b) shows the corresponding reflected grid in the complex plane ζ''. Figures 6 shows GO and PO radiation patterns in the symmetry plane assuming that the antenna is operating at 0.9 GHz, 1.8 GHz and 7.2GHz (reflector diameters of 12λ, 24λ and 96λ, respectively). Figures 7 and 8 show the PO radiation patterns at 1.8 GHz.

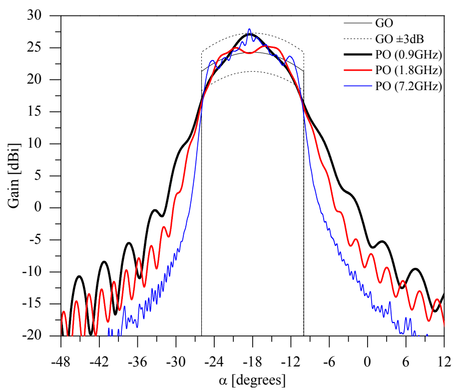

Fig. 6. Radiation patterns in the symmetry plane $\phi = 0$

V. Conclusions

This work presented a numerical method for the GO synthesis of offset reflector antennas based on the use local confocal quadric surfaces. The procedure was used to shape a reflector radiating a Gaussian pattern within a circular contour. Different from the method that uses DF, the procedure presented calculates the Jacobin matrix $J^{(n)}$ in exact analytical form, providing rapid convergence and stability. The method proved to be effective and quite flexible to be applied with other types of grids with little effort.

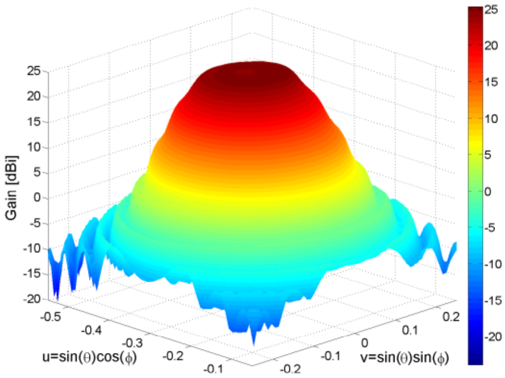

Fig. 7. Radiation pattern at 1.8GHz

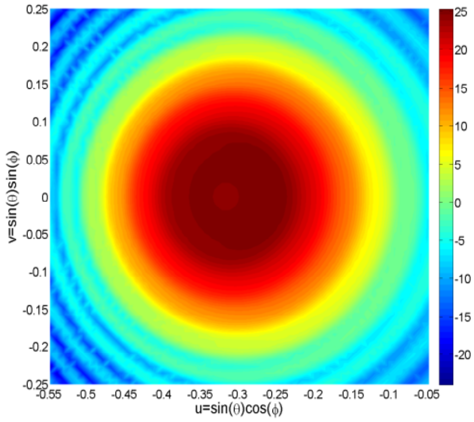

Fig. 8. Radiation pattern at 1.8 GHz in the uv-plane

Acknowledgments

This work has been partially financed by the Brazilian agencies CNPq and CAPES.

References

[1] Y. Kim and T.-H. Lee, “Shaped Circularly Symmetric dual reflector Antennas by Combining Local Conventional Dual Reflector Systems,” IEEE Trans. Antennas Propagat., vol. 57, no.1, pp. 47-56, Jan. 2009.

[2] F. J. S. Moreira and J. R. Bergmann, “Shaping Axis-Symmetric Dual-Reflector Antennas by Combining Conic Sections," IEEE Trans. Antennas Propagat., vol. 59, no.3, pp. 1042-1046, Mar. 2011.

[3] R. A. Penchel, J. R. Bergmann, and F. J. S. Moreira, "Main-Reflector Shaping of Omnidirectional Dual Reflectors Using Local Conic Sections," IEEE Trans. on Antennas and Propagat., vol. 61, no.8, pp. 4379-4383, Aug. 2013.

[4] B. S. Westcott and A. P. Norris, “Reflector Synthesis for Generalized Far-Fields,” J. Phys. A: Math. Gen., vol. 8, n. 4, pp. 521-532, Apr. 1975.

[5] F. Brickell, L. Marder and B. S. Westcott, “The Geometrical Optics Design of Reflectors Using Complex Coordinates,” J. Phys. A: Math. Gen., vol. 10, no.2, pp. 245-260, Feb.1977.

[6] B. S. Westcott, F. A. Stevens and F. Brickell, “GO Synthesis of Offset Dual Reflector,” IEE Proc. H, Microwaves, Optics and Ant., vol. 128, no.1, pp. 11-18, Feb. 1981.

[7] B. S. Westcott, R. K. Graham and I. C. Wolton, "Synthesis of Dual-Offset Shaped Reflectors for Arbitrary Aperture Shapes Using Continuous Domain Deformation," IEE Proc. H, Microwaves, Ant. and Propag., vol. 133, no.1, pp. 57-64, Feb. 1986.

[8] B. Chantraine-Bares, R. Sauleau, L. Le Coq and K. Mahdjoubi, "A New Accurate Design Method for Millimeter-Wave Homogeneous Dielectric Substrate Lens Antennas of Arbitrary Shape," IEEE Trans. on Antennas and Propagation, vol.53, no.3, pp.1069-1082, Mar. 2005